Supporting Information

Fully Bio-Based Phytic Acid-Basic Amino Acid Salt for Flame Retardant Polypropylene

Shuang He[a, b], Yu-Yang-Gao[b, c], Ze-Yong Zhao[b, c], Sheng-Chao Huang[b, c], Zi-Xun Chen[b, c], Cong Deng[b, e*], Yu-Zhong Wang[b, c, d*]

[a] *School of Chemical Engineering, Sichuan University, Chengdu 610064, China*

[b] *the Collaborative Innovation Center for Eco-Friendly and Fire-Safety Polymeric Materials, National Engineering Laboratory of Eco-Friendly Polymeric Materials (Sichuan), Sichuan University, Chengdu 610064, China*

[c] *College of Chemistry, Sichuan University, Chengdu 610064, China*

[d] *State Key Laboratory of Polymer Materials Engineering, Sichuan University, Chengdu 610064, China*

[e] *Analytical & Testing Center, Sichuan University, Chengdu 610064, China*

Figures and Tables

Figure S1. Size distribution curves of PaArg (a), PaLys (b), and PaHis (c).

Figure S2. XRD patterns of raw materials (arginine, lysine, and histidine) (a) and salts (PaArg, PaLys, and PaHis) (b) as well as phytic acid (b).

Figure S3. TG curves of raw materials (arginine, lysine, and histidine) (a) and salts (PaArg, PaLys, and PaHis) (b) under nitrogen atmosphere.

Figure S4. Burning behaviors of pure PP, PP/$PaArg_{25}$, PP/$PaLys_{25}$, and PP/$PaHis_{25}$ under the oxygen concentration of 25.0%.

*Corresponding author: Cong Deng and Yu-Zhong Wang

E-mail address: dengcong@scu.edu.cn (C. Deng); yzwang@scu.edu.cn (Y.-Z. Wang).

Figure S5. HRR (a), SPR (b), CO_2P (c), and COP (d) of PP, PP/$PaArg_{25}$, PP/$PaLys_{25}$, and PP/$PaHis_{25}$ versus time in cone calorimeter test.

Figure S6. MLR plots of PP, PP/$PaArg_{25}$, PP/$PaLys_{25}$, and PP/$PaHis_{25}$ in CONE test.

Figure S7. Absorbance of the hydrocarbons of pure PP, PP/$PaArg_{25}$, PP/$PaLys_{25}$, and PP/$PaHis_{25}$ versus time.

Table S1 TGA data of raw materials (arginine, lysine, and histidine) and salts (PaArg, PaLys, and PaHis)

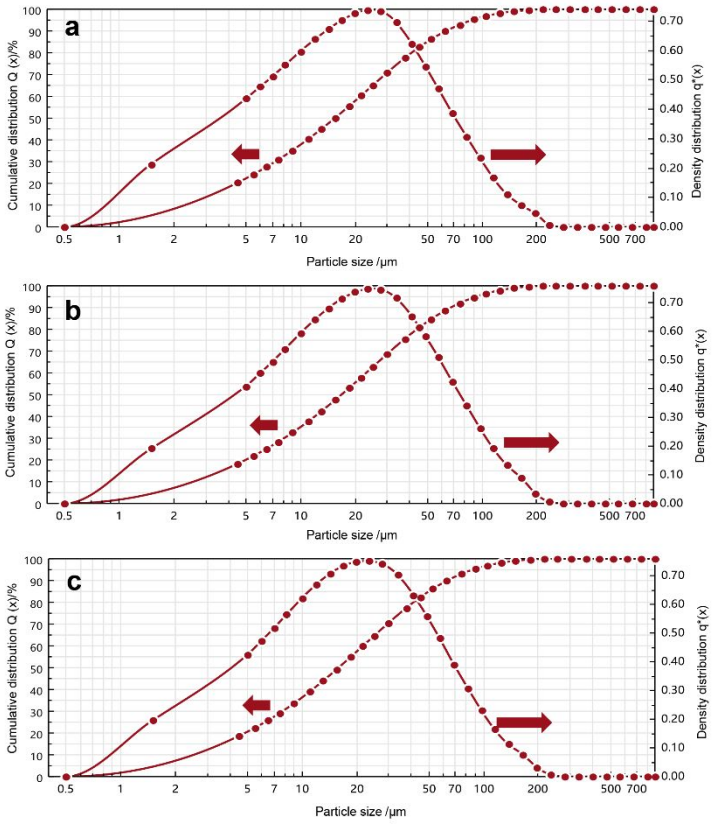

Figure S1. Size distribution curves of PaArg (a), PaLys (b), and PaHis (c).

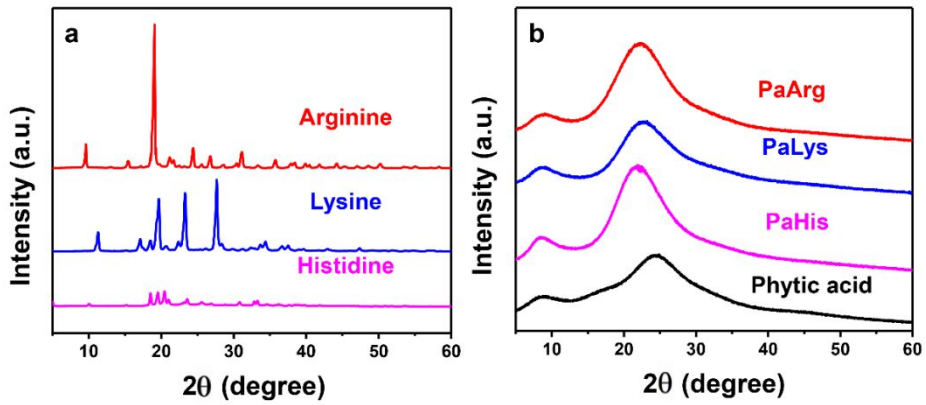

Figure S2. XRD patterns of raw materials (arginine, lysine, and histidine) (a) and salts (PaArg, PaLys, and PaHis) (b) as well as phytic acid (b).

Figure S2 shows the XRD patterns of arginine, lysine, histidine, PaArg, PaLys, PaHis, and phytic acid. In **Figure S2a,** many sharp diffraction peaks exist for each basic amino acid, indicating that basic amino acids exist in the form of crystal. In **Figure S2b**, phytic acid shows a board peak in the 2θ range from 20 to 30°, illustrating that phytic acid is almost amorphous.[1] For PaArg, PaLys, and PaHis, there is no sharp and obvious diffraction peak, illustrating that the crystalline structures of amino acids were destroyed after reaction with phytic acid, and the formed phytic acid-amino acid salts almost exist in the form of amorphous structure.

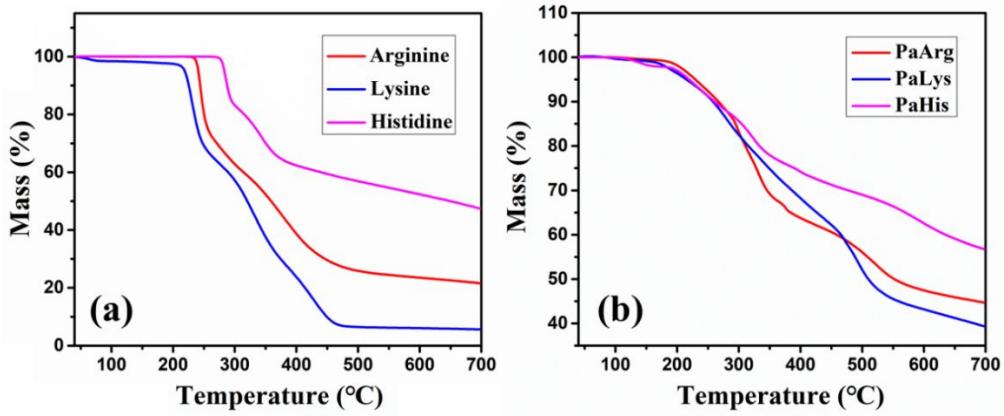

Figure S3. TG curves of raw materials (arginine, lysine, and histidine) (a) and salts (PaArg, PaLys, and PaHis) (b) under nitrogen atmosphere.

TG result of raw materials (arginine, lysine, and histidine) and salts (PaArg, PaLys, and PaHis) are shown in **Figure S3** and **Table S1**. For three kinds of amino acids, histidine has the highest $T_{5\%}$ (the temperature at 5.0 wt% mass loss), indicating that histidine has higher thermal stability than arginine and lysine. Moreover, both $T_{10\%}$ and $T_{50\%}$ (the temperatures at 10.0 and 50.0 wt% mass loss) of histidine are also higher than the corresponding values of arginine and lysine. At 700 ℃, the residue of histidine Is 47.4%, also higher than that of arginine or lysine, illustrating that histidine possess a high char-forming ability. For lysine, it shows the worst char-forming ability in three kinds of amino acids, and its residue is only 5.6% at 700 ℃, which should be due to the side group with an aliphatic chain structure. After reacting with phytic acid, the obtained three kinds of salts show a lower $T_{5\%}$ compared with the corresponding amino acids, which should be due to the low decomposition temperature of phytic acid.[2] However, both $T_{10\%}$ and $T_{50\%}$ are higher than the corresponding values of amino acid. For example, $T_{50\%}$ value for PaArg is increased by 53.7% compared with that of arginine. For PaHis, the final residue even exceeds 50%, showing an excellent char-forming ability. More interestingly, the residue of PaLys reaches 39.33%, greatly increased by 598.6% in comparison with that of lysine, showing the highest synergic efficiency with phytic acid in forming char. Clearly, PaHis has a different decomposing behavior from PaArg and PaLys. The former is much more thermal stable than the latter two at high temperature. TG result indicates that both amino acid and phytic acid played a synergistic effect in forming stable char, which might be contribute to the formation of the char with high thermal stability after the initial thermal decomposition. In addition, the decomposition temperature scope of the used PP is about 401-480 ℃ in this work, while the main decomposition

temperature range of three flame retardants is 220-460 ℃. Therefore, the pyrolysis range of the bio-based flame retardant is consistent with that of PP.

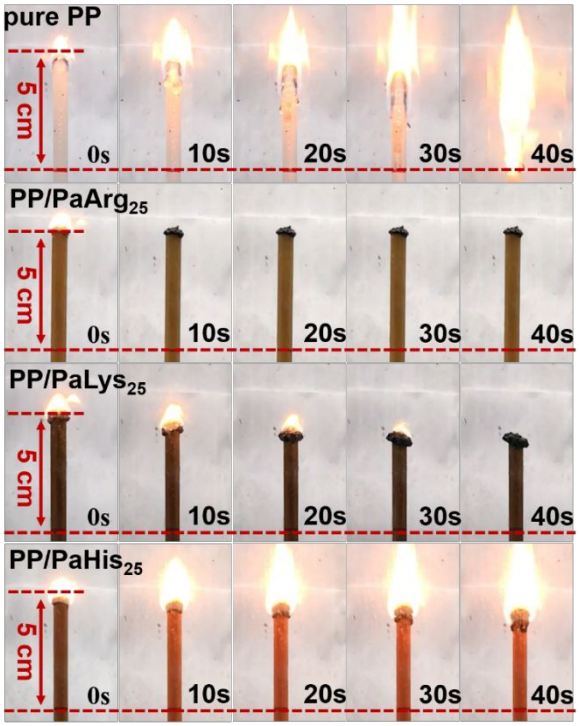

Figure S4. Burning behaviors of pure PP, PP/PaArg$_{25}$, PP/PaLys$_{25}$, and PP/PaHis$_{25}$ under the oxygen concentration of 25.0%.

The burning processes of pure PP, PP/PaArg$_{25}$, PP/PaLys$_{25}$, and PP/PaHis$_{25}$ under the same oxygen concentration of 25.0% are shown in **Figure S4**. The combustion of pure PP was extremely fierce, and the burnt length reached to 5 cm within 40 s. For PP/PaArg$_{25}$, the flame extinguished quickly within 10 s and only a small portion of the sample was burnt. PP/PaLys$_{25}$ self-extinguished at about 30 s and the burnt length was only about 1 cm. For PP/PaHis$_{25}$, the flame did not extinguish at 40 s, showing poor flame retardancy. In summary, the PaArg, PaLys, and PaHis showed an apparent difference in flame-retardant efficiency, and both PaArg and PaLys displayed higher charring ability than PaHis during burning.

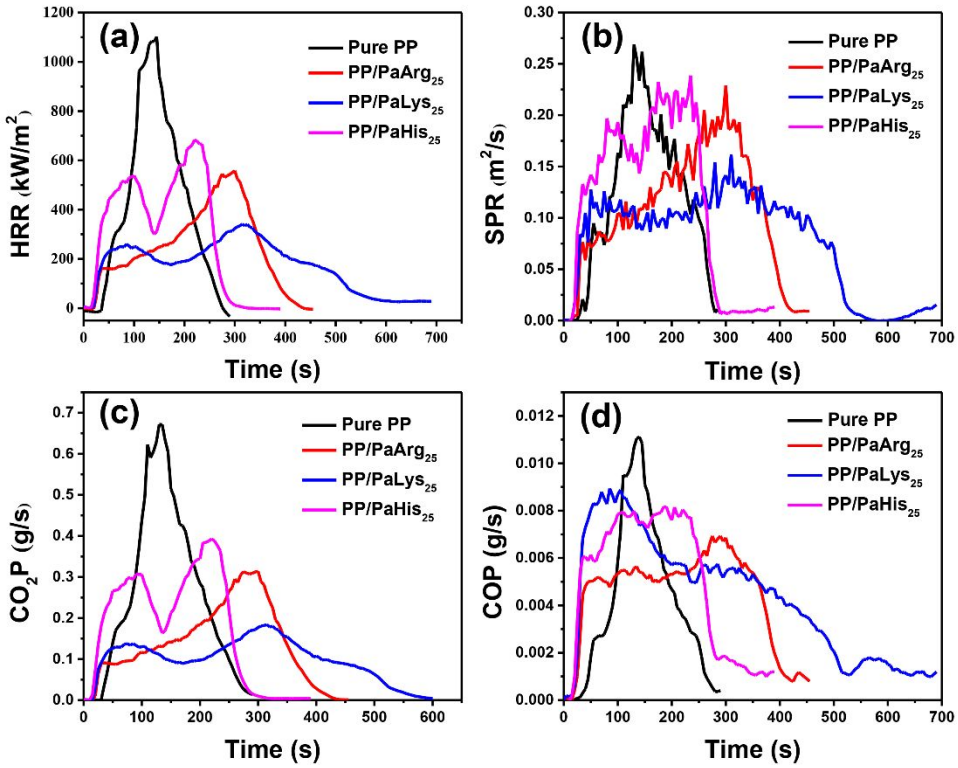

Figure S5. HRR (a), SPR (b), CO_2P (c), and COP (d) of PP, PP/PaArg$_{25}$, PP/PaLys$_{25}$, and PP/PaHis$_{25}$ versus time in cone calorimeter test.

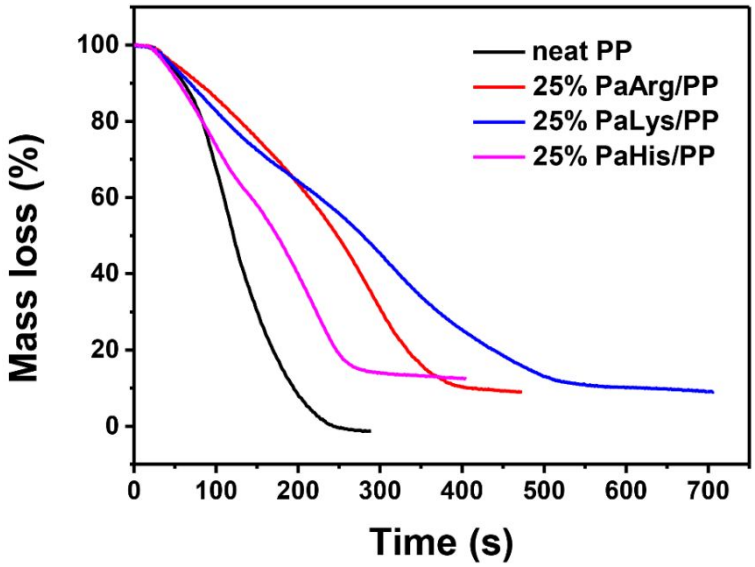

Figure S6. MLR Plots of PP, PP/PaArg$_{25}$, PP/PaLys$_{25}$, PP/PaHis$_{25}$ in CONE test.

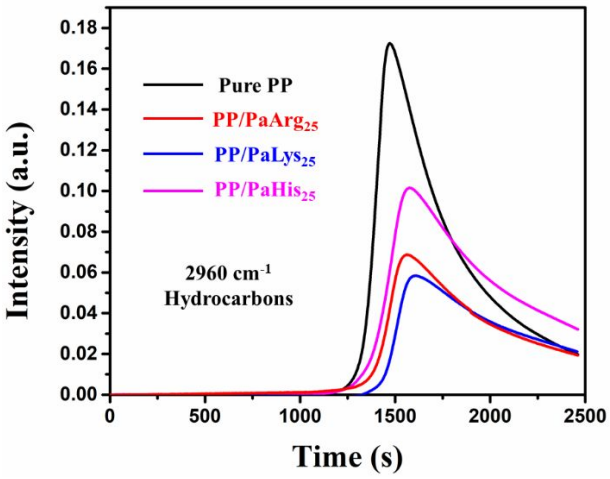

Figure S7. Absorbance of the hydrocarbons of pure PP, PP/PaArg$_{25}$, PP/PaLys$_{25}$, and PP/PaHis$_{25}$ versus time.

Table S1 TGA data of raw materials (arginine, lysine, and histidine) and salts (PaArg, PaLys, and PaHis)

Sample	$T_{5\%}$ (℃)	$T_{10\%}$ (℃)	$T_{50\%}$ (℃)	*Residue at 700 ℃* (%)
Arginine	240.9	243.8	358.9	21.6
Lysine	219.0	225.5	320.3	5.6
histidine	283.3	287.6	649.9	47.4
PaArg	229.4	267.1	551.8	44.7
PaLys	215.2	261.1	509.8	39.3
PaHis	219.4	551.8	\	56.7

References

1. Zhang, T.; Yan, H.; Shen, L.; Fang, Z.; Zhang, X.; Wang, J.; Zhang, B., Chitosan/Phytic Acid Polyelectrolyte Complex: A Green and Renewable Intumescent Flame Retardant System for Ethylene–Vinyl Acetate Copolymer. *Ind. Eng. Chem. Res.* **2014,** *53* (49), 19199-19207.

2. Cheng, X.-W.; Guan, J.-P.; Chen, G.; Yang, X.-H.; Tang, R.-C., Adsorption and Flame Retardant Properties of Bio-Based Phytic Acid on Wool Fabric. *Polymers* **2016,** *8* (4), 122.